Fluid theory of the boundary of a dusty plasma

J. X. Ma and Jin-yuan Liu
Department of Modern Physics, University of Science and Technology of China, Hefei, Anhui 230027, China

M. Y. Yu
Institut für Theoretische Physik I, Ruhr-Universität Bochum, D-44780 Bochum, Germany

(Received 18 June 1996; revised manuscript received 23 September 1996)

The motion and distribution of charged dust grains under the action of electrostatic and gravitational forces near the boundary of a dusty plasma are investigated. It is shown that when gravity is negligible, a spatial localization of the dust can occur. For heavier grains, gravity enhances this localization, and causes a stratification of the dust density. For even heavier grains, the stratification disappears since the grains are pulled to the wall by gravity. [S1063-651X(97)01804-7]

PACS number(s): 52.40.Hf, 52.25.Vy, 52.35.Sb, 52.55.Dy

I. INTRODUCTION

Dust particles are frequently observed in space [1–4] and laboratory [5–11] plasmas. In the past several years, much attention has been paid to collective effects in dusty plasmas [12–20]. Dust grains are often found to be localized near the plasma boundary where the electrostatic (ES) force balances the gravitational and other forces [21]. They can also coagulate [22,23] or form Coulomb crystals [24–26]. Heavily charged dust particles can thus significantly modify the structure of the boundary plasma.

The wall region of two-component plasmas has been qualitatively understood for many years [27]. Recently, the ES sheath of dusty plasmas was studied for dynamic dust grains with constant charge [28], as well as for stationary dust grains with variable charge [29]. In both cases, the gravitational force on the dust is ignored, so that the existing results are applicable only for very light grains or at walls which are in the vertical (parallel to gravity) direction. However, in many realistic situations the dust grains are heavy, and the region of interest is perpendicular to gravity, so that the latter can play a significant role on the dynamics of the grains. In the present paper, we study the dust dynamics in the wall region by taking into consideration both the ES and gravitational forces on the variable-charge grains. It is found that gravity can cause a strong stratification as well as localization of the dusts near the plasma boundary. Furthermore, if the sheath size is sufficiently large, the region immediately adjacent to the wall can be completely depleted of electrons, and the dust grains can eventually become positively charged there.

We use the standard fluid model [27] for the sheath, treating the plasma electrons as hot Boltzmann particles, and the ions and dusts as cold fluids. The variable dust charge is determined self-consistently by the plasma currents collected at the grain. In Sec. II, the formulation of the boundary problem is presented. In Sec. III, we study the case of small (light) grains, for which gravity can be neglected. The effect of gravity on the sheath structure is investigated in Sec. IV. Our results are summarized and discussed in Sec. V.

II. FORMULATION

We consider the wall region of a one-dimensional stationary ($\partial_t = 0$) plasma. The electrons are assumed to be hot and in thermal equilibrium. The ions and dust grains, whose temperatures are usually much lower than that of the electrons, are assumed to be cold. The variable dust charge is determined by the electron and ion currents entering the grain, as governed by the potential difference between the grain surface and the local plasma. Other effects, such as secondary-electron and photoelectron currents associated with possible high-energy electrons and intense UV radiation, will not be considered.

The bulk plasma, which includes both the presheath and source regions, is located in $x \leqslant 0$, and is assumed to be quasineutral. The details of this region, including sources, particle acceleration by a weak presheath electric field, and the gravitational action on the dusts, are not considered here. The region of interest lies between $x = 0$, where the potential is taken to be zero, and the wall. The location of the wall can be anywhere in the region $x > 0$, and is determined by the wall potential or other boundary conditions.

The density of the thermal electrons is

$$n_e = n_{e0} \exp(e\phi / T_e), \tag{1}$$

where ϕ is the ES potential, e the electron charge, T_e the electron temperature, and n_{e0} the electron density at the sheath edge $x = 0$. In the following, the subscript 0 shall denote quantities evaluated at $x = 0$.

The ions, treated as a cold fluid, are accelerated in the presheath region to a mean velocity v_{i0} at $x = 0$ by a weak presheath electric field. In the absence of dusts, it is well known that v_{i0} must exceed the ion acoustic speed $c_{is} = (T_e / m_i)^{1/2}$ in order for the sheath solution to exist [27]. Using the continuity and the momentum conservation equations, the ion density can be expressed as [27]

$$n_i = n_{i0} \left(1 - \frac{2e\phi}{m_i v_{i0}^2} \right)^{-1/2}, \tag{2}$$

where m_i is the ion mass.

The dust grains are collectively treated as a cold fluid. Possible forces on a dust grain are electrostatic, gravitational, as well as ion and neutral particle drag [21]. The ES force is proportional to the grain radius in the probe model because of the linear dependence of the grain charge on radius. The gravitational force is proportional to the cube of the radius. The ion and neutral particle drag forces are proportional to the square of the grain radius as well as the ion and neutral fluxes. Thus the ES force is dominant for small grains, while, for heavier grains, gravity can have an appreciable effect on the dust dynamics. The ion and neutral drag forces could be effective for large grains and high plasma densities, but they shall not be considered here. We assume that the dust grains are accelerated to a velocity v_{d0} at $x=0$ by the electric and gravitational forces in a presheath region. Thus the conservation equations for the dust are

$$n_d v_d = n_{d0} v_{d0}, \tag{3}$$

$$m_d v_d d_x v_d = -q_d d_x \phi + m_d g, \tag{4}$$

where g is the gravitational acceleration, and m_d and v_d are the mass and mean velocity of the dusts, respectively. In the above, we assumed that gravity is toward the wall, although for the opposite case one only needs to change the sign of g.

The dust charge q_d is determined by equation

$$v_d d_x q_d = I_e + I_i, \tag{5}$$

which describes charge conservation. The charging currents originate from electrons and ions hitting the grain surface. According to the orbit-limited probe model [21,30], the electron and ion currents I_e and I_i flowing into the grains are determined by local electron and ion densities, as well as the potential difference between the grain surface and the local plasma. The grain current from the Boltzmann electrons is [1,21]

$$I_e = -\pi r^2 e \left(\frac{8T_e}{\pi m_e} \right)^{1/2} n_e W_e(q_d), \tag{6}$$

and that from the cold ions is [21]

$$I_i = \pi r^2 e n_i v_i \left(1 - \frac{2eq_d}{r m_i v_i^2} \right), \tag{7}$$

where r is the grain radius, $W_e(q_d)=\exp(eq_d/rT_e)$ when $q_d<0$, and $W_e(q_d)=1+eq_d/rT_e$ when $q_d>0$. We note that the characteristic time for dust motion is of the order of tens of milliseconds for micrometer-sized grains [18], while the dust charging time, or that for the grain to be charged from zero to the (relative to the ambient plasma) floating potential, is typically of the order of 10^{-8} s [31]. Within the time of charging, the displacement of the grain is thus negligible compared to the spatial scale of the problem. It follows that the charging process can be treated as a local phenomenon, and the convective term on the left-hand side of Eq. (5) can be neglected. That is, we have $I_e+I_i=0$, and the grains are always at the floating potential.

The system is completed by the Poisson equation

$$d_x^2 \phi = -4\pi [e(n_i - n_e) + n_d q_d], \tag{8}$$

and the neutrality condition

$$e(n_{i0} - n_{e0}) + n_{d0} q_{d0} = 0 \tag{9}$$

for the unperturbed plasma at $x=0$.

For simplicity, we introduce the dimensionless quantities $\Phi=-e\phi/T_e$ and $Q_d=eq_d/rT_e$, and normalize the x coordinate $X=x/\lambda_e$ with respect to the electron Debye length $\lambda_e=(T_e/4\pi e^2 n_{e0})^{1/2}$. We also define the ion and dust Mach numbers $M_j=v_{j0}/c_{js}$, where $j=i,d$. $c_{ds}=(zT_e/m_d)^{1/2}$ is the dust acoustic speed [12], and $z=rT_e/e^2$ is the dust charge number at $Q_d=1$ (i.e., when the floating potential on the grain surface is T_e/e). In addition, we define the dimensionless ''potential energy'' of the grain in the ES field,

$$\Psi = \int_0^{\Phi} Q_d d\Phi,$$

which leads to a considerable simplification of the formulation. Accordingly, the densities can be written as

$$N_e = \frac{n_e}{n_{e0}} = \exp(-\Phi), \tag{10}$$

$$N_i = \frac{n_i}{n_{i0}} = \left(1 + \frac{2\Phi}{M_i^2} \right)^{-1/2}, \tag{11}$$

$$N_d = \frac{n_d}{n_{d0}} = \left(1 + \frac{2\Psi}{M_d^2} + \frac{2\mu}{M_d^2} X \right)^{-1/2}, \tag{12}$$

where $\mu = g\lambda_e/c_{ds}^2$ is a measure of the gravitational effect. The Poisson equation becomes

$$d_X^2 \Phi = -N_e + fN_i - (f-1) N_d Q_d / Q_{d0}, \tag{13}$$

where $f=n_{i0}/n_{e0}$ is the ratio of ion-to-electron density at the sheath edge.

As mentioned, the dust charge is determined by equating the electron and ion grain currents (6) and (7). With the help of Eqs. (10) and (11), the relation between the potential and dust charge can be written as

$$\Phi = -\tfrac{1}{2} M_i [M_i - \alpha f (M_i^2 - 2Q_d') \exp(-Q_d')] \tag{14}$$

for $Q_d<0$, and

$$Q_d = \frac{(2\phi + M_i^2)[\alpha f M_i - \exp(-\Phi)]}{2\alpha f M_i + (2\Phi + M_i^2)\exp(-\Phi)} \tag{15}$$

for $Q_d>0$, where $Q_d' \equiv Q_d - \Phi$, and $\alpha=(\pi m_e/8m_i)^{1/2}$ is a coefficient which is approximately 0.0146 for a hydrogen plasma.

The function Ψ for $Q_d<0$ can be obtained analytically with the help of Eq. (14), yielding

$$\Psi = \tfrac{1}{2} \{ \Phi^2 + \alpha f M_i [G(Q_d') - G(Q_{d0})] \}, \tag{16}$$

where $G(y) \equiv [(M_i^2 - 2y)(1+y) - 2]\exp(-y)$, and we used the condition $\Phi=0$ and $Q_d=Q_{d0}$ at $X=0$. For $Q_d>0$, Ψ can be obtained by numerically integrating Eq. (15). The

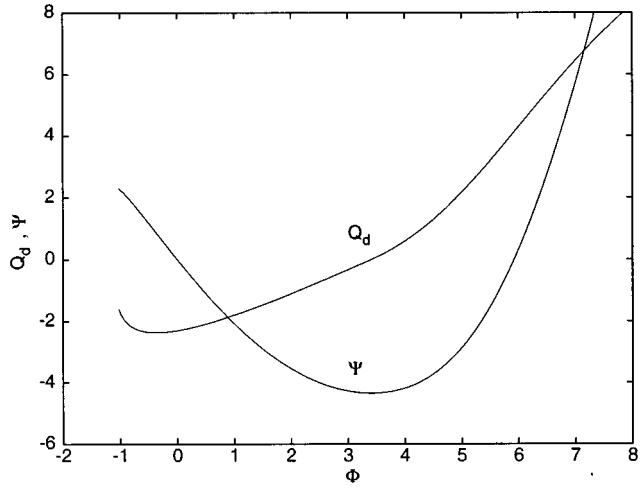

FIG. 1. Variation of the normalized charge Q_d and ES energy Ψ of the dust with respect to the normalized ES potential Φ for $f=1.5$ and $M_i=1.5$.

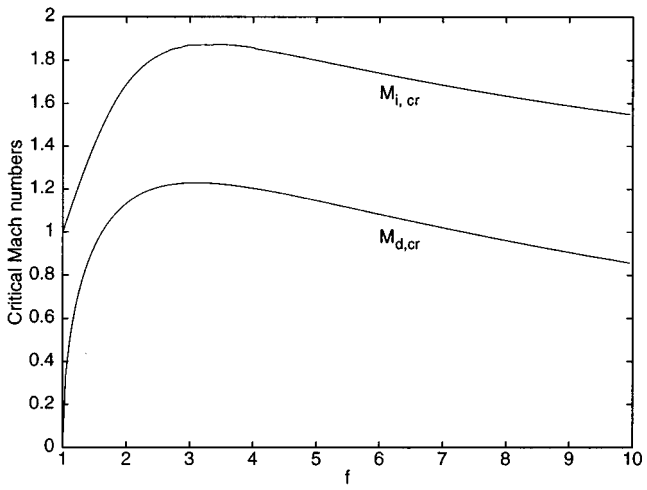

FIG. 2. The critical ion and dust Mach numbers vs the ion-to-electron density ratio $f=n_{i0}/n_{e0}$. Here $M_d=2.5$ for the M_i curve, and $M_i=1.5$ for the M_d curve.

variation of Q_d and Ψ vs Φ is given in Fig. 1, which shows that Q_d increases monotonically with $\Phi>0$, while Ψ decreases monotonically with Φ, until Q_d becomes positive and the electron density vanishes.

Equations (10)–(13) form a complete set of ordinary differential equations for the sheath problem. They are highly nonlinear, and are exact within the basic assumptions. However, because of the explicit dependence of N_d on the coordinate X, one cannot in general obtain a quadrature. A rough estimate of relative importance of the ES and gravitational forces can nevertheless be made by looking at Ψ and the coefficient μ in Eq. (12). For an argon plasma, the magnitude of the dimensionless dust charge Q_{d0} is around 3.9. Since the dimensionless ES potential Φ is of the order of 1, the function Ψ is of the order of 4. On the other hand, the magnitude of μ is given by $\mu=2.74\times10^3 r^2\rho_d T_e^{-3/2} n_{e0}^{-1/2}$, where ρ_d is the mass density of a grain in units of g cm^{-3}, and r and T_e are in units of μm and eV, respectively. If we take $\rho_d\sim3$ g cm^{-3}, $T_e\sim1$ eV, and $n_{e0}\sim10^9$ cm^{-3}, we have $\mu=0.26r^2$. Thus, for micrometer-sized grains, gravity is comparable to the ES force at a distance of $X=10$, and will dominates over the ES force if X is a few decades further toward the wall. Since μ is proportional to r^2, gravity quickly becomes the dominant effect in determining the dust dynamics when the grain radius exceeds a few micrometers. In the following, we shall consider the sheath structures with and without gravity separately.

III. SMALL PARTICLES

In this section, the dust particles are assumed to be small (light), such that the gravitational force is negligible (i.e., $\mu X\ll\Psi$ for the region of interest). In this case, Eqs. (10)–(13) can easily be integrated to the quadrature,

$$(d_X\Phi)^2+2V(\Phi)=E_0^2, \tag{17}$$

where E_0 is a possible small presheath electric field and is taken to be effectively zero here. The pseudopotential (or Sagdeev potential) $V\equiv V_e+V_i+V_d$ consists of

$$V_e=1-\exp(-\Phi), \tag{18}$$

$$V_i=-fM_i^2[(1+2\Phi/M_i^2)^{1/2}-1], \tag{19}$$

$$V_d=\frac{(f-1)}{Q_{d0}}M_d^2\left[\left(1+\frac{2\Psi}{M_d^2}\right)^{1/2}-1\right], \tag{20}$$

which represent the contributions from the electrons, ions, and dust particles, respectively.

The potential Φ is obtained by integrating Eq. (17) from $\Phi=0$ to the (floating) wall potential, which determines the location of the wall. Prior to the numerical solution it is instructive to look at the properties of the sheath structure by analyzing the Sagdeev potential. We first note that bounds for Φ exist. The lower bound is $\Phi=-M_i^2/2$, at which the ion density becomes infinity. The upper bound is determined by $\Psi=-M_d^2/2$, which corresponds to an infinite dust density. Using a small-amplitude analysis, the condition $d_\Phi^2 V\leqslant0$ at $\Phi=0$ for the existence of a solution requires the ion and dust Mach numbers to satisfy

$$M_i^2\geqslant M_{i,\mathrm{cr}}^2\equiv[-B+(B^2-4AC)^{1/2}]/2A \tag{21}$$

and

$$M_d^2\geqslant M_{d,\mathrm{cr}}^2\equiv(f-1)Q_{d0}^2/(f-1-Q_{d0}), \tag{22}$$

where $A=1+(f-1)Q_{d0}(M_d^{-2}-Q_{d0}^{-2})$, $B=2A(1-Q_{d0})-f+2(f-1)/Q_{d0}$, and $C=-2f(1-Q_{d0})-4(f-1)$. Note that for $f=1$, corresponding to the dust-free case, one obtains $M_{d,\mathrm{cr}}=0$ and $M_{i,\mathrm{cr}}=1$, which is consistent with the Bohm criteria for a two-component plasma [27]. Figure 2 gives the ion and dust critical Mach numbers as functions of the ion-to-electron density ratio f. We see that both $M_{i,\mathrm{cr}}$ and $M_{d,\mathrm{cr}}$ first increase and then decrease with f. The fact that $M_{i,\mathrm{cr}}>1$ means that there must exist a larger accelerating field in the presheath region than that in the dust-free case in order for the ions to acquire the energies needed to overcome the ES dragging of the slow dust particles.

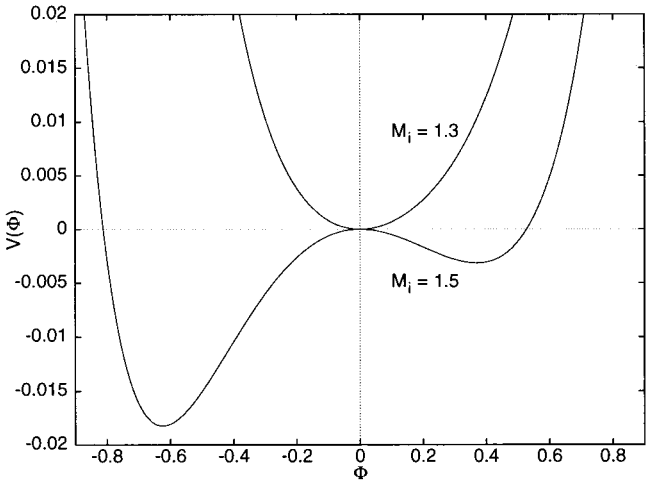

FIG. 3. The Sagdeev potential $V(\Phi)$ vs Φ for $f=1.5$ and $M_d=2.7$, at two different M_i values.

Figure 3 shows two typical Sagdeev potentials for $f=1.5$, $M_d=2.7$, and $M_i=1.3$ and 1.5. The critical ion Mach number here is about 1.4. For the case $M_i=1.3$ ($<M_{i,\mathrm{cr}}$), it is clear that no solution can exist (for $E_0=0$). For $M_i=1.5$ ($>M_{i,\mathrm{cr}}$), a double well structure appears. It is well known [27], and is obvious from Eqs. (18)–(20) that, without the dust contribution ($V_d=0$) the Sagdeev potential for $\Phi>0$ is monotonically decreasing. Thus, we see that the well structure on the right side of Fig. 3 is caused by the dusts.

The solution is obtained by integrating Eq. (17). To start the numerical integration, a small edge electric field $d_X\Phi(0)=0.001$ associated with the presheath is assumed. The ES potential Φ and the densities N_e, N_i, and N_d are given in Fig. 4, which exhibits a spatially localized (solitonlike) structure, as is evident from the well structure of the Sagdeev potential in Fig. 3. The peak value of Φ corresponds to the right zero of $V(\Phi)$ in Fig. 3. Note the particularly strong localization of the dust. A similar behavior of the

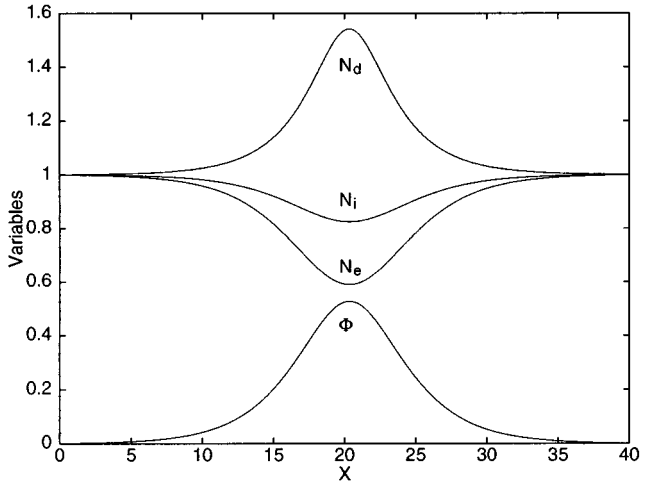

FIG. 4. The normalized ES potential Φ, and the electron, ion, and dust densities N_e, N_i, and N_d vs $X=x/\lambda_e$ for the case of no gravitation. The parameters are $f=1.5$, $M_i=1.5$, and $M_d=2.7$.

particles is observed for other parameter values. The localization is caused by a balance of the ES forces on the grains. Since near the sheath edge ($X=0$) the force is directed toward the unperturbed plasma or presheath region, it tends to decelerate the grains (which are moving toward the wall), and cause their accumulation within the sheath. The accumulated grains in turn contribute to a negative ES field which eventually offsets the positive field, leading to a dust density maximum. The localized dust grains act as a virtual wall for the electrons and ions. In the absence of field-aligned gravitational forces or particle drag, this virtual wall is symmetric on both sides, so that the solution exhibits a solitonlike spatial profile [32].

IV. EFFECT OF GRAVITATION

When gravitation is included in Eq. (12), the method in Sec. III fails, since the corresponding Sagdeev potential cannot be obtained. However, for not too large grains near the sheath edge such that $\mu X\ll 1$, we can still use a similar analysis to understand the qualitative behavior of the Φ variation near $X=0$. Accordingly, in this limit the dust contribution (20) to the Sagdeev potential can be approximated by

$$V_d\approx\frac{(f-1)M_d^2}{Q_{d0}}\left[\left(1+\frac{2(\Psi+\mu X)}{M_d^2}\right)^{1/2}-1\right], \qquad (23)$$

which depends explicitly on X, and is analogous to a time-dependent Hamiltonian system. Since $Q_{d0}<0$ and $\Psi<0$ (Fig. 1), we conclude that except when the electrons are depleted gravitation tends to decrease the value of V_d. Thus the right potential well would be deepened as X increases, and steeper profiles (stronger localization) of Φ and N_d would appear.

We have numerically integrated Eq. (13), assuming an argon plasma with $T_e=1\mathrm{eV}$, $n_{e0}=10^9\ \mathrm{cm}^{-3}$, and dust grains of mass density $\rho=3\ \mathrm{g/cm}^3$. The results are presented in Figs. 5–7. The sheath profiles depend on the grain size as well as the parameters f, M_i, and M_d. In addition to the stronger localization of the dust, asymmetric oscillatory structures are observed for medium-sized grains and a wide range of parameter values. Figure 5, in which $r=1\mu\mathrm{m}$, $f=1.5$, $M_i=1.5$, and $M_d=1.8$, shows that a strong multipeak structure of N_d appears, with the maximum value of the last peak at $N_d\sim 20$. The corresponding ES potential Φ increases in an oscillatory manner, while the electron and ion densities decrease in a similar manner [Fig. 5(b)]. We observe that the electron density is depleted after some distance. The dust charge can also become locally positive when the corresponding Φ becomes sufficiently large (see Fig. 1). After the last peak, the dust density rapidly drops to zero, leaving a pure ion sheath. Similar profiles are obtained for other parameter values and grain radii, with either stronger or weaker multipeaks. Figure 6, for smaller grains $r=0.5\mu\mathrm{m}$ and with $f=1.4$, $M_i=1$, and $M_d=2.5$, shows a case of oscillatory behavior with weaker peaks. It is of interest to point out that these dust profiles resemble those observed experimentally in Refs. [5] and [6].

The multilayer structure, corresponding to a stratification of the dust fluid, is the result of competition between the ES

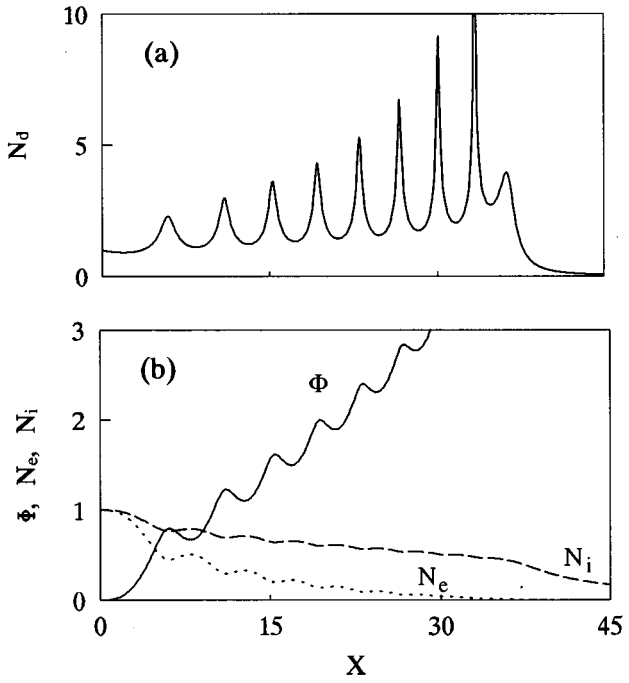

FIG. 5. The distributions of (a) dust density and (b) the ES potential and electron and ion densities vs X for the case including gravitational effects. The grain radius is $r=1\mu$m and the other parameters are the same as Fig. 4 except $M_d=1.8$.

and gravitational forces. Physically, the phenomena can be understood as follows. The variation of the dust density with respect to X is given by

$$dN_d/dX=-N_d^3M_d^{-2}(Q_d d_X\Phi+\mu), \tag{24}$$

where the last two terms represent the ES and gravitational effects, respectively. For a given grain size, the gravitational force is a constant, but the ES force varies according to the (self-consistent) sheath potential and the dust charge. The two effects balance ($Q_d d_X\Phi+\mu=0$) at the density minima and maxima. Near the sheath edge $X=0$, the ES force is

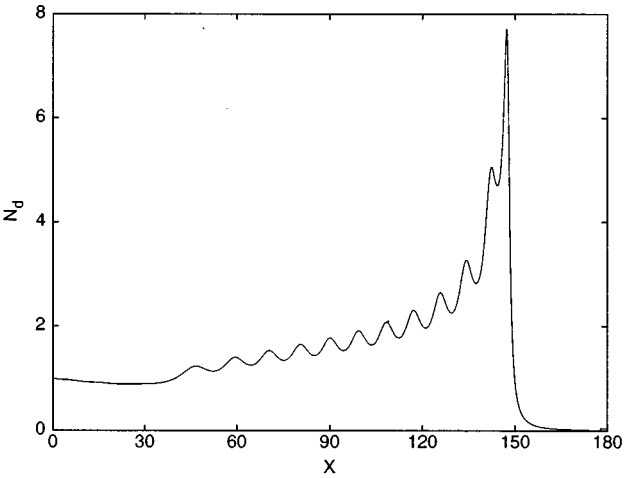

FIG. 6. The profile of the dust density vs X for a case with grain radius $r=0.5\mu$m, $f=1.4$, $M_i=1$, and $M_d=2.5$.

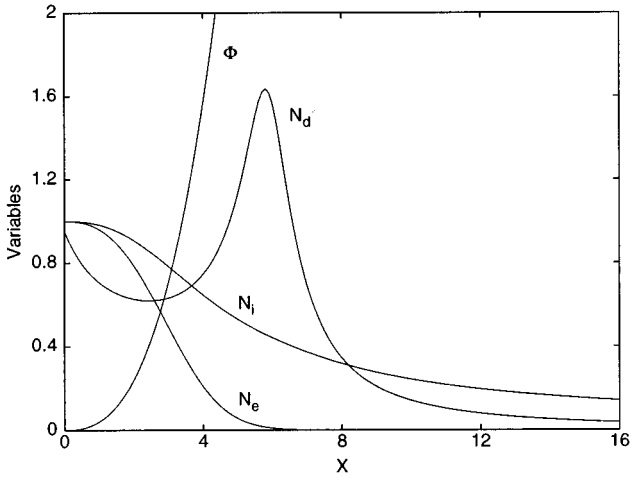

FIG. 7. Same as Fig. 5, except here $r=2.5\mu$m.

small and the grains are accelerated by gravity toward the wall. This is in contrast to the gravity-free case, and leads to a local decrease of N_d near $X=0$. Away from the edge, the (negatively charged) grains experience an increasing ES force which is in the opposite direction, thus reducing the acceleration. Still further into the sheath the two forces eventually balance, leading to a minimum in N_d. After this point, the ES force exceeds that of gravity and decelerates the grains, leading to accumulation of the latter. However, the accumulation of the negatively charged dusts reduces the local ES field (consisting of a positive part arising from the charge separation of electrons and ions, and a negative part from the dusts), which in turn causes a reduction of the accumulation. Thus an N_d maximum occurs. After that, N_d again decreases because of the gravity and the ES force (the local ES field can even become negative) until it reaches the next minimum. This process repeats until the wall (determined by conditions there) is reached or electrons become depleted. Since gravity is unidirectional, the system cannot resume the initial state after each peak despite the absence of friction. Because of the rapid reduction of electrons as X increases, a more negative ES field (thus more dust accumulation) is required to counter the positive field from the ions in the sheath. Therefore, each succeeding peak is higher than the previous one. Clearly, the fact that the charge Q_d becomes less (more) negative as Φ increases (decreases) contributes to the sharpness of the peaks.

With an increase of the grain radius, the number of peaks in the sheath decreases until only one peak remains, followed by a rapid decrease of the dust density. Such a structure is shown in Fig. 7, where $r=2.5\mu$m. Note that in this case the electron density is quickly depleted, leaving an ion and dust sheath. Furthermore, as a result of strong charge separation very large electric fields appear. This causes the grain charge to increase and eventually become positive. Thus the ES force decreases, and can eventually change its direction (so that it is the same as that of gravity). In this case, both forces pull the grains toward the wall, leading to the abrupt drop in the dust density (see Fig. 7). At even larger grain radii, the single peak is eventually smoothed out. Furthermore, the dust density rapidly drops to zero, so that a pure ion sheath appears. The latter phenomenon occurs because for large

grains (or for sufficiently large X as in the cases of Figs. 5 and 6), the gravitational force, which now dominates over the ES force, rapidly accelerates the dust grains to the wall.

V. SUMMARY AND DISCUSSION

In this paper, we investigated the ES sheath structure at the boundary of a typical dusty plasma by considering the hydrodynamic motion of heavy dust grains under the ES and gravitational forces. It was shown that for small grains, for which gravity is negligible, the sheath profile resembles a soliton with highly localized dust density. For medium-sized grains, an interplay of the ES and gravitational forces causes a multilayer structure, or stratification of the dust. For still larger grains, due to the dominance of gravity over the ES force, the stratification disappears and the localization weakens, as the grains are rapidly pulled to the wall. It should also be noted that, although away from $x=0$ the ion density is larger than the dust density, because of the large charge number the dust charge can still dominate in determining the total electric field. It is therefore appropriate to refer to such a region as a dust sheath. However, if the wall is very far from $x=0$ (as determined by the wall conditions), the dusts can vanish. In this case the usual ion sheath remains. The dust distributions found here are in qualitative agreement with the experimentally observed phenomenon of dust localization [5,6,33]. The results here may also be relevant to the phenomena of dust-particle growth [34,35] and dust-crystal formation [25,26], since the regions of intense dust localization provide favorable conditions for the latter.

Our analysis of dust dynamics is based on the continuous medium model which requires sufficiently many dust particles within the characteristic length. Our results indicate that the characteristic spatial scale of the dust sheath is of the order of a few electron Debye lengths λ_e. Roughly, the continuous medium model holds if $d<\lambda_e$, where $d=n_d^{-1/3}$ is the intergrain distance. Thus, the present analysis is valid for $n_d>\lambda_e^{-3}$. On the other hand, the dust charging model, i.e., the orbit-limited probe model for the charging currents, is restricted to at most one grain in the Debye sphere. This requires d to be larger than the ion Debye length λ_i. Therefore, the present study is applicable for $\lambda_e^{-3}<n_d<\lambda_i^{-3}$. For example, for a plasma with $n_e\approx n_i=10^9\ \mathrm{cm}^{-3}$, $T_e=1$ eV, and $T_i=0.1$ eV, the dust density must satisfy $7.7\times10^4<n_d<2.4\times10^6$ (in cm^{-3}). In general, if the dusts are too rarefied or too dense, one has to use a discrete model for the dusts, or take into account charge correlation between neighboring grains, respectively.

We have not included ion drag and neutral collision forces on the dust grains, both of which can play a role [21,36], especially in the regions of dust enhancement. Depending on the ion density and grain radius, the ion drag force may be comparable to gravity. Thus, we expect that the ion drag can enhance the effect of gravity. The neutral collision force, on the other hand, depends on the gas flow and pressure, and can be significant if there is a large gas flux.

ACKNOWLEDGMENTS

We thank C. X. Yu for fruitful discussions. This work was supported by the International Atomic Energy Agency (Contract 8933/Regular Budget Fund), the National Natural Science Foundation of China, the Postdoctoral Science Foundation of China, and the USTC Youth Science Foundation. The work of M.Y.Y. was partially supported by the Sonderforschungsbereich 191 Niedertemperaturplasmen.

[1] E. C. Whipple, Rep. Prog. Phys. **44**, 1198 (1981).
[2] E. C. Whipple, T. G. Northrop, and D. A. Mendis, J. Geophys. Res. **90**, 7405 (1985).
[3] C. K. Goertz, Rev. Geophys. **27**, 271 (1989).
[4] T. G. Northrop, Phys. Scr. **45**, 475 (1992).
[5] G. Selwyn, J. Singh, and R. S. Bennet, J. Vac. Sci. Technol. A **7**, 2758 (1989).
[6] K. G. Spears, T. J. Robinson, and R. M. Roth, IEEE Trans. Plasma Sci. **14**, 179 (1986).
[7] M. Hunhausen and L. Ley, J. Non-Cryst. Solids **137-138**, 795 (1991).
[8] W. Böhme, W. E. Köhler, M. Römheld, S. Vepřek, and R. J. Seeböck, IEEE Trans. Plasma Sci. **22**, 110 (1994).
[9] R. J. Seeböck, W. Böhme, W. E. Köhler, M. Römheld, and S. Vepřek, Plasma Sources Sci. Technol. **3**, 354 (1994).
[10] S. Robertson, Phys. Plasmas **2**, 2200 (1995).
[11] B. Walch, M. Horanyi, and S. Robertson, Phys. Rev. Lett. **75**, 838 (1995).
[12] N. N. Rao, P. K. Shukla, and M. Y. Yu, Planet. Space Sci. **38**, 543 (1990).
[13] V. N. Tsytovich and O. Havnes, Comments Plasma Phys. Control. Fusion **15**, 267 (1993).
[14] R. K. Varma, P. K. Shukla, and V. Krishan, Phys. Rev. E **47**, 3612 (1993).
[15] M. R. Jana, A. Sen, and P. K. Kaw, Phys. Rev. E **48**, 3930 (1993).
[16] S. V. Vladimirov, Phys. Rev. E **49**, 997 (1994); Phys. Plasmas **1**, 2762 (1994).
[17] J. X. Ma and M. Y. Yu, Phys. Plasmas **1**, 3520 (1994); Phys. Rev. E **50**, 2431 (1994).
[18] A. Barkan, R. L. Merlino, and N. D'Angelo, Phys. Plasmas **2**, 3563 (1995).
[19] J. X. Ma, P. K. Shukla, and M. Y. Yu, Phys. Lett. A **198**, 357 (1995); J. X. Ma and P. K. Shukla, Phys. Plasma **2**, 1506 (1995).
[20] P. K. Shukla and S. V. Vladimirov, Phys. Plasma **2**, 3179 (1995).
[21] M. S. Barnes, J. H. Keller, J. C. Forster, J. A. O'Neill, and D. K. Coultas, Phys. Rev. Lett. **68**, 313 (1992).
[22] V. A. Schweigert and I. V. Schweigert, J. Phys. D **29**, 655 (1996).
[23] S. V. Vladimirov and M. Nambu, Phys. Rev. E **52**, 2172 (1995); S. V. Vladimirov and O. Ishihara, Phys. Plasmas **3**, 444 (1996).
[24] H. Ikezi, Phys. Fluids **29**, 1764 (1986).
[25] J. H. Chu and Lin I, Phys. Rev. Lett. **72**, 4009 (1994).
[26] H. Thomas, G. E. Morfill, V. Demmel, J. Goree, B. Feuerbacher, and D. Möhlmann, Phys. Rev. Lett. **73**, 652 (1994).

[27] F. F. Chen, *Introduction to Plasma Physics* (Plenum, New York, 1974), Chap. 8.

[28] M. Y. Yu, H. Saleem, and H. Luo, Phys. Fluids B **4**, 3427 (1992).

[29] J. X. Ma and M. Y. Yu, Phys. Plasmas **2**, 1343 (1995).

[30] F. F. Chen, in *Plasma Diagnostic Techniques*, edited by R. H. Huddlestone and S. L. Leonard (Academic, New York, 1965), Chap. 4.

[31] D. Winske and M. E. Jones, IEEE Trans. Plasma Sci. **23**, 188 (1995).

[32] In fact, the Sagdeev potential (17) has a structure similar to that in the nonlinear dust acoustic wave theory [12], which also predicts soliton formation. It is of interest to point out that soliton splitting similar to those found in Sec. IV are known for (weak) solitons in inhomogeneous media [37].

[33] C. Steinbrüchel, in *Plasma Sources for Thin Film Deposition and Etching*, edited by M. H. Francombe, and J. L. Vossen (Academic, San Diego, 1994), p. 289.

[34] G. M. W. Kroesen, W. W. Stoefels, E. Stoffels, M. Haverlag, J. H. W. G. den Boer, and F. J. de Hoog, Plasma Sources Sci. Technol. **3**, 246 (1994).

[35] Y. Watanabe and M. Shiratani, Plasma Sources Sci. Technol. **3**, 286 (1994).

[36] J. F. O'Hanlon, J. Kang, L. K. Russell, and L. Hong, IEEE Trans. Plasma Sci. **22**, 122 (1994).